Proceedings of IPACK2005
ASME InterPACK '05
July 17-22, San Francisco, California, USA

IPACK2005-73221

MULTIDIRECTIONAL FORCE AND TORQUE SENSOR FOR INSECT FLIGHT RESEARCH

Mansoor Nasir [a], Michael Dickinson [b] and Dorian Liepmann [a]
[a] Dept. of Bioengineering, Berkeley Sensors and Actuator Center, University of California, Berkeley
497 Cory Hall #1774, Berkeley CA 94720-1774
[b] Bioengineering, Mail Code 138-78 California Institute of Technology. 1200 E. California Blvd. Pasadena, CA 91125

ABSTRACT

This paper focuses on the development of a microsensor system that can simultaneously measure multidirectional forces generated by a tethered fly. The proposed sensor combines the well-understood concepts of piezoresistive force sensing with a very unique design that not only allows the measurement forces with more than one degree of freedom (DOF) but will simultaneously support the fly inside a virtual reality arena. The sensor is fabricated on a wafer-level using standard MicroElectro-Mechanical System or MEMS technology. By a directly measuring the thrust, lift, yaw and side slip generated by the fly, complex aerodynamics mechanisms due to rapidly rotating and flapping wings can be better understood.

INTRODUCTION

Flying insects have developed sophisticated and unrivalled flight mechanisms permitting them a remarkable range of maneuvers. Flight is not simply a means of transport but many insects use aerial acrobatics to capture prey, defend territories and acquire mates [1]. Fruit flies (*Drosphila melanogaster)* are a popular model for biologist and for insect flight research as they have pushed the envelope of organismal design. Within flies, we find the fastest visual systems, the most powerful muscles, a wing hinge of mind-boggling complexity, and a pair of wings that outrival any modern gyroscope. The feedback-mediated flight circuitry of the fly, which enables it to effortlessly execute elaborate aerial maneuvers represents a control system of extraordinary speed and robustness, far exceeding the capabilities of any existing robots. Thus, flies represent a superb model system for elucidating general principles that govern complex biological systems. These principles are no doubt critical in the realization of any biomemtics inspired flying microrobotic systems.

ROLE OF FORCE SENSING IN UNDERSTANDING UNSTEADY AERODYNAMIC PRINCIPLES

It is a known fact that insect flight incorporates unsteady aerodynamic principles, which are extremely complex due to the rapidly rotating and flapping wings that generate flight forces varying in time and space. Of particular interest to the biologists are the lift, thrust and yaw forces applied by the fruit fly (Fig. 1).

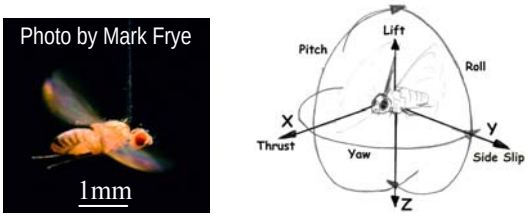

Fig. 1: (Left) A fruit fly tethered to a Tungsten rod. Generally adult female flies are used and weigh 2—5mgm. (Right) The forces along different axes from the viewpoint of a fly.

By being able to measure these forces simultaneously, different flight maneuvers and the neural, sensory and mechanical feedbacks that affect the flight motor control, can be better understood.

A significant problem has been that insect flight must be intuited from differential wing beat frequency and amplitude measurements. Dickinson et. al use optical methods to track *tethered* fruit flies inside a virtual reality arena (Fig 2.) to make these measurements.

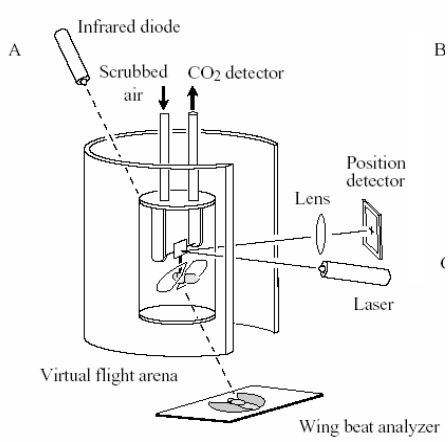

Fig. 2: *Flyorama* or LED flight arena developed Dickinson et. al to study unsteady aerodynamic principles used by fruit flies in tethered flight. (See [2, 3] for more details)

Yaw force measurements were made by the angular deflection of a laser beam aimed at a small mirror mounted to the fly's tether [2]. However the measurements with laser require elaborate test setup and are prone to error since due to forces perpendicular to body axis of the fly.

MEMS technology by combining integrated-circuit microfabrication techniques with macroscopic instrumentation principles, makes it possible to develop highly sensitive microsensor systems that are adapted to the requirements of biomimetic studies. Capacitive sensing methods have been used to measure the lift force generated by tethered fruit flies with much higher accuracy [4]. However, until now direct measurement of forces with greater than single degree of freedom (DOF) has not been possible. A MEMS sensor capable of making multidirectional force measurements can be instrumental in understanding issues like the number of independent control inputs and interactions between different forces during flight maneuvers, among others that are as of yet, not completely understood.

FORCE MICROSENSOR DESIGN

In developing a microsensor for measurement of flight forces, a number of requirements need to be satisfied. The sensor has to balance the material strength needed to support the weight of the fruit fly while at the same time remain compliant enough to measure forces less than 50μN [2]. The design should also allow for easy tethering of the fly and placement inside the *Flyorama* setup. Sensor reusability is important for reliable and repeatable test results.

The scale of forces involved are suitable to be measured using capacitive force sensors as in a comb-drive force sensor [4]. However, measuring forces with more than one DOF, with a tethered fly using capacitive sensing techniques is not possible due to size limitations. The number of transducers needed to simultaneously measure both rotational and translational forces would make the sensor too big and fabrication exceedingly complicated.

Another popular mechanism for force measurements is to use piezoresistive strain gauges. Piezoresistivity a material property due to which the resistance changes when stress is applied. Strain gauges have been used for quite sometime and probably the most common type have a metal foil patterned on to a flexible polymer backing. The gauge is bonded on to a surface such that when the underlying surface is strained, it deforms the strain gauge as well and causes a change in its resistance. The change in resistance is measured, most frequently, by using a Wheatstone bridge configuration (Fig. 4).

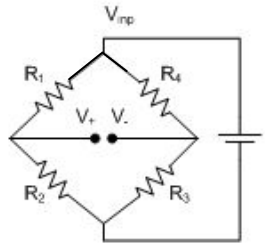

Fig. 4: Wheatstone bridge shown above can be used in quarter, half or full configurations depending upon the number of active elements in the four legs of the circuit.

The bridge is initially balanced with the strain gauges in the circuitry. As the resistance of the strain gauge changes, the bridge becomes unbalanced and an output voltage results. The change in voltage can be related to strain using a quantity known as the *gauge factor*. Semiconductor strain gauges measure small strains much more effectively as they have a higher gauge factor, typically anywhere from 10—50 times more than their metallic counterparts [5]. They can be microfabricated with high precision and bypass the issues related to bonding and have therefore, been used extensively in MEMS engineering applications. Recently strain gauge sensors have been used in biological applications such as the forces generated by cockroaches while walking and running [6].

We have designed a sensor design that uses piezoresistive strain gauges to measure the flight forces of interest i.e. lift, thrust and yaw, in real time (Fig. 3).

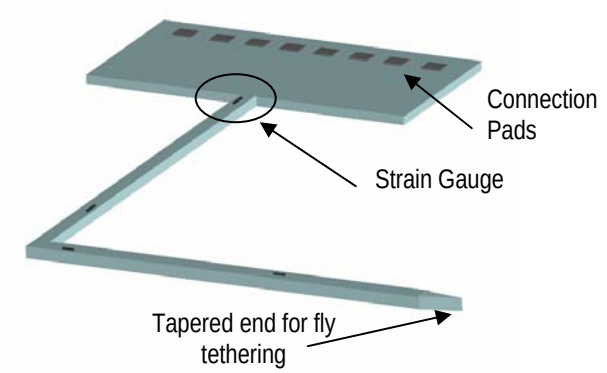

Fig. 3: A model of force microsensor. The fly is tethered at the tapered end of the L-shaped sensor.

The novel design allows replaces the current fly tether and is capable of simultaneously supporting the fly inside the fly arena and measuring the rotational and translational forces. Our design has four strain gauges that are used in quarter bridge configuration. The wide base acts like an anchor and also has contact pads to measure the voltage across the strain gauges.

ANALYTICAL MODEL

Linear beam theory can be used to find the governing equations defining the relation between the forces acting at the tip of the sensor and resulting strain across each strain gauges. The base of the sensor is essentially an anchor and is eventually glued to a PCB therefore the acting forces only deform the L-shaped structure of the sensor. The three forces, lift (F_L), Thrust (F_T) and Yaw (M_{yaw}) are shown to be acting at the bottom end of the vertical beam where the fly is tethered during flight experiments.

With a free body diagram all the moments resulting from these forces can be visualized (Fig. 5). Using a force-moment analysis the moment along z-axis at any point 'y' along the length of the vertical beam of length L_V, is given by

$$M_z(y) = M_{VT} - F_T.y = F_T.(L_V - y) \qquad (1)$$

where M_{VT} is the moment due to thrust force F_T on the vertical beam.

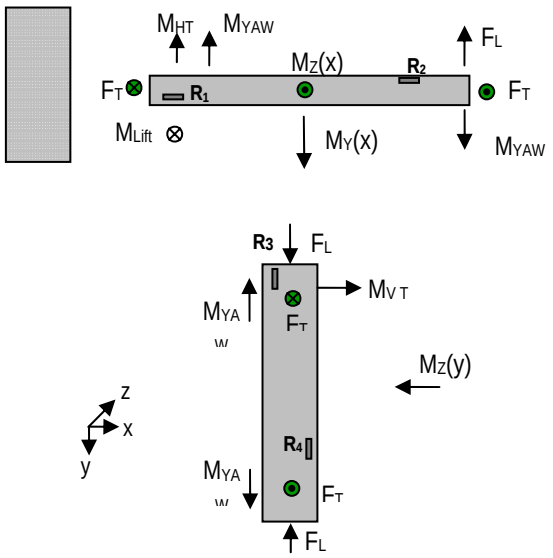

Fig. 5: Free body diagram of the force sensor. The lengths of the vertical and horizontal beams are L_V and L_H respectively. Right hand rule has been used to show the forces and moments acting on the ends of the beams.

Similarly the moments in y-axis and z-axis at any point 'x' along the length of the horizontal beam of length L_H, are given by

$$M_y(x) = M_{LIFT} - F_L.x = F_L.(L_H - x) \qquad (2)$$

$$M_z(x) = M_{YAW} + M_{HT} - F_T.x = M_{YAW} + F_T(L_H - x) \qquad (3)$$

where M_{HT} is the moment on the horizontal beam due to thrust force F_T acting on the vertical beam and M_{LIFT} is the moment due to lift force F_L acting on the vertical beam. The relationship between the stress, σ, and moments is given by

$$\sigma = \frac{M}{I}c \qquad (4)$$

where 'c' is the distance from neutral fiber and 'I' is the moment, which for a rectangular beam is given by the equation

$$I = \frac{bh^3}{12} \qquad (5)$$

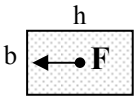

Using Hook's law, the strain, ε, can be related to the moments given by equations 1—3.

$$\varepsilon_Z(y) = \frac{F_T.(L_V - y)}{E.I_z y}c_z(y), \qquad I_z y = \frac{b^3 h_V}{12} \qquad (6)$$

$$\varepsilon_Y(x) = \frac{F_L.(L_H - x)}{E.I_y x}c_y(x), \qquad I_y x = \frac{bh_H^3}{12} \qquad (7)$$

$$\varepsilon_Z(x) = \frac{M_{yaw} - F_T.(L_H - x)}{E.I_z x}c_Z x, \quad I_z x = \frac{b^3 h_H}{12} \qquad (8)$$

where h_H and h_V are the widths of the horizontal and vertical beams respectively. Equations 6, 7 and 8 can be written down for lengths x and y that correspond to the location of four strain gauges. The different 'c' values are the distances from the respective neutral fibers. The gauge factor, G, of a strain gauge relates strain to change in electrical resistance.

$$\varepsilon = \frac{1}{G}\frac{\Delta R}{R} \qquad (9)$$

Thus the resistance of the four strain gauges can be related to the forces and moments acting on the beams. Using eq. 6—9 the change in resistance (and therefore voltage) of all four strain gauges due to forces applied can be found.

	R_1	R_2	R_3	R_4
F_T	↑	↑	↑	↓
F_L	↑	↓	↔	↔
M_y	↑	↑	↔	↔

Table 1: The effects of increasing forces on the resistance of four strain gauges. By simultaneously measuring the change in resistances the forces can be resolved using equations described in this section

For the sake of simplicity, the torsional and axial stresses caused by the forces have been neglected but can be easily added for a more rigorous analytical model.

FINITE ELEMENT MODEL (FEM) OF SENSOR DESIGN

FEM analysis was done for the sensor design to validate the results from theoretical calculations using ANSYS software. Since the sensor is microfabricated out of Si substrate, the generally accepted values of 0.22 and 160GPa were used for Poisson ratio and Young's modulus respectively.

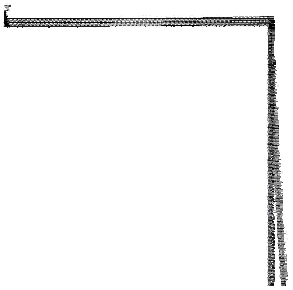

Fig. 6: The meshed L-shaped structure used to simulate the strains caused by forces applied to at the end of the vertical beam, in this case along the x-axis (thrust force).

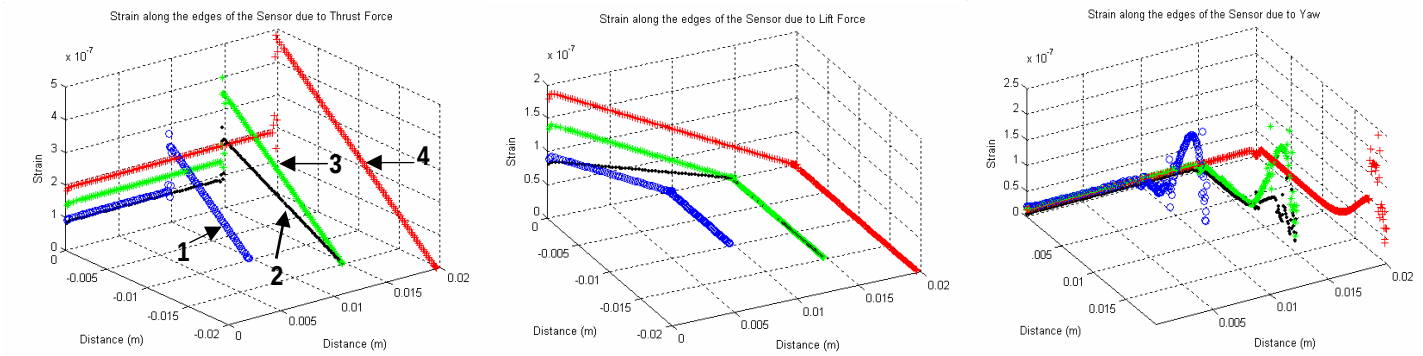

(a) (b) (c)

Fig. 7: Four variations consisted of different lengths and thicknesses of the L-shaped structure. 1 and 4 both had beam thicknesses 300µm but beam lengths were 10mm and 20mm respectively. 2 and 3 both had beam lengths of 15mm but the beam thicknesses are 300µm and 500µm respectively. For each of these cases a 10µN force was applied along the x and y axis for thrust (a) and lift (b) respectively and a 10nN-m force was applied about the y-axis for yaw simulations (c). The data files from ANSYS simulations were processes in MATLAB for analysis and plotting.

Different design variations were simulated under same conditions of force and torque (Fig. 7). Since the system was simulated under the assumption of linear elastic behavior i.e. small displacements, strain varies linearly when thicknesses and length of beams are changed. The longer the beam is the higher is the strain at a specific location. Similarly the thicker the beam is, the stiffer it is and so the lesser is the sensitivity.

According since in linear beam theory, the strain is inversely proportional to the cube of the thickness while it is only directly proportional to the length of a beam, decreasing the thickness has a much more profound effect on strain. This can be seen by comparing the total strain from variation 1 and 2. A shorter but thinner beam (#1) has a higher strain distributed along the beam as compared to a longer but thicker beam (#2).

MICROFABRICATION

Bulk micromachining has been used to fabricate the L-shaped sensor out of single crystal silicon wafer. A pair of polysilicon strain gauges are microfabricated on each arm of the sensor with aluminum leads for measuring the voltages across them. The leads connect to pads that are designed specifically for wirebonding to a printed circuit board (Fig. 8).

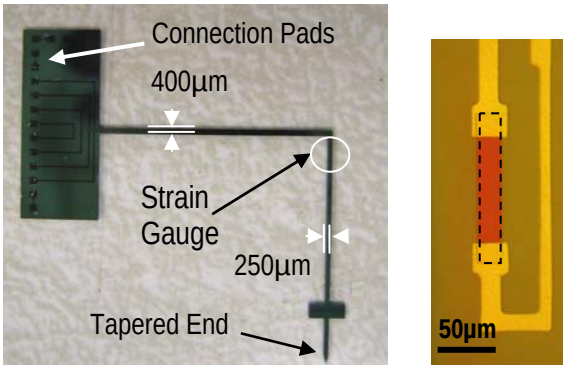

Fig. 8: (Left) Microfabricated force sensor with one of the strain gauges highlighted. (Right) a magnified view of the strain gauge and Aluminum leads.

A small overlap between the leads and the polysilicon strain gauges helps reduce the contact resistance. The fabrication of the force microsensor uses standard lithographic and etching steps and requires only three masks (Fig. 9). A larger structure will obviously be more flexible but apart from the sensors becoming too fragile, fabrication procedure also requires high precision due to the fact that extremes range of scales are involved in the dimension of the sensor; from the long cantilever arms to the strain gauges.

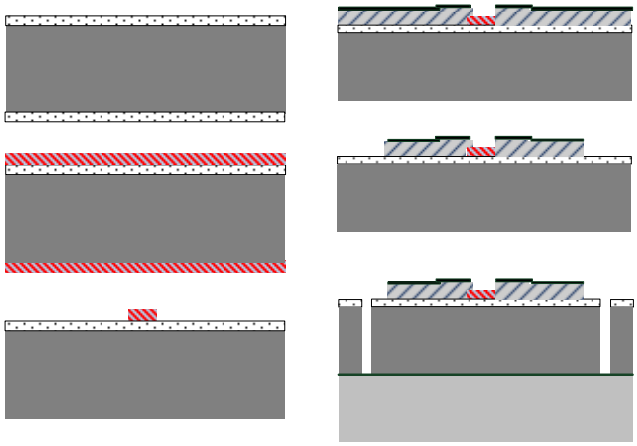

Fig. 9: Microfabrication process (a) A thin oxide layer (<1µm) is grown on a P-type single crystal Si wafer which will act as a passivation layer. (b) N-doped poly silicon layer (~400Å) is deposited on the wafer after oxide has been removed from the back side of the wafer. The polysilicon deposition step is followed by an annealing step to drive in the dopants. (c) Polysilicon strain gauges are defined using an RIE etch (Mask1). (d) A thick layer of Aluminum (~1.2µm) followed by a very thin layer of Titanium (<100Å) is sputtered on the front side of the mask. The Ti layer helps protect the Al leads from getting scratched off. (e) The following lithographic step defines the leads (Mask2). The leads are etched with a combination of dry and wet etches. (f) After a handle bond is attached a last lithographic step (Mask3) is used to RIE etch oxide around the boundaries of the wafer followed by a DRIE through-etch from the front side.

PROTOTYPE SENSOR CALIBRATION

Initial testing of the sensor with static loads has been done. Each strain gauge is held in a quarter Wheatstone bridge. A signal conditioning amplifier (OMEGA OM-161K) completes the bridge and also amplifies and filters the output voltage of the bridge. Trimpots can be used to adjust the bridge output voltage to zero when the beam is unstrained. A force transducer is used to apply a known force at the tip of the sensor and the change in voltage is measured simultaneously across the four strain gauges (Fig. 10). The whole test setup is placed inside a closed hood to prevent the voltage fluctuations due to air drafts and temperature variations.

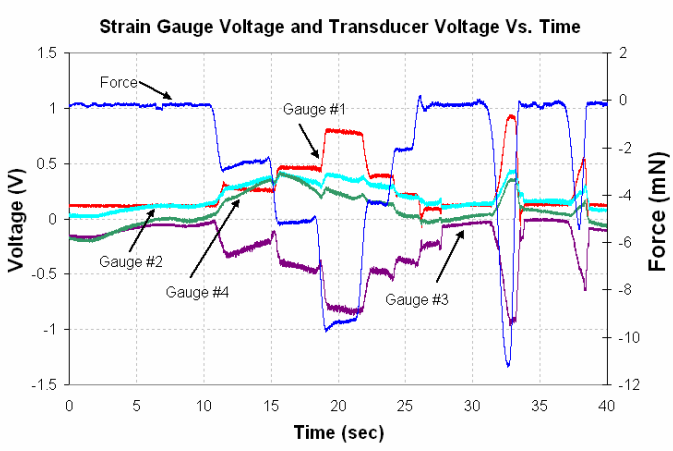

Fig. 10: Change in voltage in all four strain gauges when lift force is applied (with the transducer) at the tip of the sensor. Gauge #1 is stretched so its resistance increases where as for Gauge #2 and #4 are not very responsive. The increase in Gauge #3 is due to the stress at the elbow in trying to keep the vertical arm in its position when being pushed up by the transducer.

The results for static forces show that the strain gauge voltages vary almost linearly with the applied force (Fig. 11).

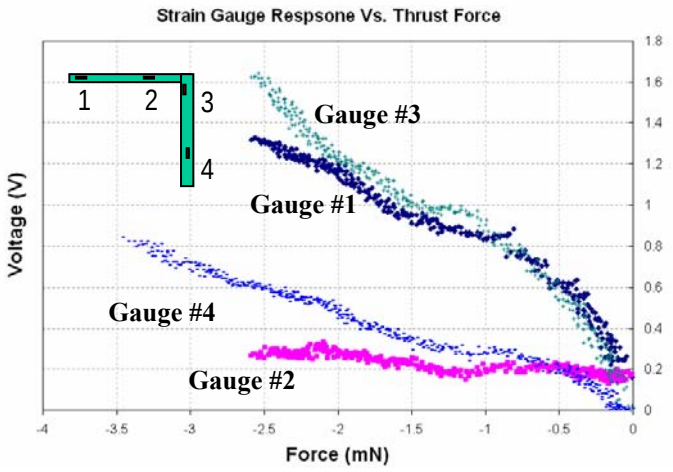

Fig. 10: Change in voltage as a function of applied force shows a nearly linear relationship. The result is shown for all four strain gauges. As expected the force, thrust in this case produces a different degree of response in the strain gauges depending on their location and strain gradient in the arms of the sensor.

Similar response has been measured for the lift and yaw. By tethering the fly at 90°, thrust force can be substitute for the side-slip force response. In order to measure the smallest possible force, precision weights were hung from the tip of the sensor. Force as small as 100μN have been successfully measured with sensors fabricated out of 300μm thick wafers. The dynamic response is also under investigation currently.

DISCUSSION

The research is in the calibration phase of the sensor but in order to measure the forces generated by fruit flies in particular, the sensitivity has to be increased further. Measuring forces smaller than 100μN has not been possible with the current design. As seen from ANSYS simulation results a tethered fruit fly exerts forces so small that the resulting strains are roughly in tenths of a μ-strain range. This means that the sensor has to not only be quite sensitive but error generating effects of temperature drifts, lead resistance and self-heating of the strain gauge need to be accounted for as well.

One simple method to increase sensitivity is to make the whole sensor much more flexible by using thinner wafer. A fabrication run with thinner wafers was recently processed. Sensors were fabricated out of 100μm thick wafers and could measure forces as small as 50μN. However it is very easy to break the wafer during the process and so using wafers thinner than 300μm is not a particularly viable option. A better option is thin the sensor locally around the area where strain gauges are microfabricated. This is currently being done by doing a backside etch on the wafer before sensors are released. New sensors with this change are currently being processed and will be tested against the sensors with uniform thickness to see the increase in strain when same force is applied at the tip of the sensor.

Semiconductor strain gauges are attractive since they are much more sensitive than metal foil strain gauges. However, metal foil strain gauges show significantly less drift due to temperature fluctuations as compared to semiconductor strain gauges. It is for this reason that semiconductor strain gauges are almost always used in a full or a half-bridge unless they are being operated in a stable temperature environments. For temperature compensation the sensors are being used in a half bridge configuration in which a dummy strain gauge in added to the bottom leg of the side with active strain gauge. Thus if the temperature fluctuates, the voltage drifts equally in both active and dummy strain gauges and the temperature drift effect are therefore greatly minimized.

CONCLUSION

A force microsensor system has been developed. The novel design of the sensor allows measurement of forces with greater than single DOF that are being applied by a fly tethered to one end of the sensor. Initial testing of the sensor has verified the proof of concept and forces as small as 100μN have been successfully measured. The sensor will be used in tethered fly experiments inside a virtual LED arena and by measuring multidirectional forces in real time, complex aerodynamics mechanisms due to rapidly rotating and flapping wings can be better understood.

ACKNOWLEDGMENTS

The researchers would like to thank Packard Foundation for funding this project.

REFERENCES

[1] Dickinson, M. H. "*Solving the Mystery of Insect Flight."* **Scientific American**, June 17th 2001

[2] Dickinson, M. H. and Lighton, J. R. B. "*Muscle Efficiency and Elastic Storage in the Flight Motor of Drosophila"* **Science**, April 7th 1995, Vol. 268, p. 87—90.

[3] Lehmann, F.-O. and Dickinson, M. H. "*The Changes in Power Requirements and Muscle Efficiency during Eleveated Force Production in the Fruit Fly* Drosophila Melanogaster." **The Journal of Experimental Biology**, 1997, 200, p. 1133—1143.

[4] Potassek DP, Sun Y, Fry SN and Nelson BJ. "*Characterizing fruit fly flight behavior using a micro force sensor with a new comb drive configuration.*" **J. of MEMS**, February 2005, Vol. 14, p 4—11.

[5] Strain gauge technology. A. L. Window. 2nd ed. Chapter 6, 7 & 8. 1992.

[6] Bartsch, M. S., Partridge, A., Pruitt, B. L., Full. R. J. and Kenny, T. W. "*A Three-Axis Piezoresistive Micromachined Force Sensor for Studying Cockroach Biomechanics.*" **MEMS, ASME,** 2000**,** Vol. 2, p. 443—448.